

PROCEEDINGS OF SPIE

SPIDigitalLibrary.org/conference-proceedings-of-spie

New opportunities of freeform gratings using diamond machining

Cyril Bourgenot, Ariadna Calcines, Ray Sharples

Cyril Bourgenot, Ariadna Calcines, Ray Sharples, "New opportunities of freeform gratings using diamond machining," Proc. SPIE 10706, Advances in Optical and Mechanical Technologies for Telescopes and Instrumentation III, 1070626 (11 July 2018); doi: 10.1117/12.2312040

SPIE.

Event: SPIE Astronomical Telescopes + Instrumentation, 2018, Austin, Texas, United States

New opportunities of freeform gratings using diamond machining

Cyril Bourgenot^a, Ariadna Calcines^a, Ray Sharples^a

^aDurham University, Department of Physics, Centre for Advanced Instrumentation, NETPark Research Institute, Joseph Swan Road, Sedgefield, TS21 3FB, UK;

ABSTRACT

With the recent development of new ultrafine aluminium alloys and progress in the field of directly machined freeform surfaces, diamond machined freeform gratings could play an important part in future spectrographs or integral field units, particularly at SWIR and LWIR wavelengths where the improved thermal performance of metal optics at cryogenic temperatures is well established. Freeform diamond machined gratings can offer a cost-effective, compact, and flexible alternative to gratings fabricated by other methods such as ion beam etching or complement these technologies. In this paper, both the advantages and limitations of 5 axis diamond machined freeform gratings are presented and potential applications are discussed.

Keywords: Diamond turning, tool servo, freeform optics, precision machining

1. INTRODUCTION

The development of diffraction gratings for the next generation of spectrographs is facing tremendous challenges. With 3 giant telescopes currently under construction (ELT,¹ TMT² and GMT³) and their first light instruments being at various stages of design, the choice of technology for the dispersive element is now being carefully compared. The future spectrographs will be equipped with large and high efficiency gratings enabling unique spectral performance offered by the exceptional resolving power of these giant telescopes. Different diffraction gratings technologies have been selected:

- Volume Phase Holographic gratings (VPHG) for the 10 dispersive elements of HARMONI⁴ and for GMT's near-infrared Spectrograph GMTIFS and GMACS^{5,6}.
- Silicon immersion grating for the Mid-infrared E-ELT imager and spectrograph METIS⁷ and for GMT's Near-Infrared Spectrograph GMTNIRS⁸.
- Ruled gratings for TMT's IRIS spectrograph⁹
- Replication of ruled gratings for GMT's G-CLEF¹⁰

Another manufacturing technique involving a directly etched binary profile onto silica by e-beam or ion-beam etching is currently being assessed for an UV based spectrograph for ESO CUBES UV spectrograph.¹¹ While ground-based astronomical spectrographs are pushing the technology towards larger dimensions, hyperspectral imagery for Earth Observation (EO) applications, on the other hand, requires more compact systems. For these space applications demanding compact solutions, freeform optics constitute a smart alternative, improving the instrument performance and reducing the volume. Freeform optics are novel and revolutionary¹² optical elements with no particular axis of rotation or symmetry. In particular, they can help to improve compactness, image sharpness and contrast in larger fields of view. They are therefore promising components for space-based hyperspectral imagers. Freeform gratings have been used so far in systems with low to medium spectral resolution^{13,14} and have enabled an increase of the SNR, a minimization of the volume and a good image quality over the field of view (FoV). In these examples (Refs^{13,14}), the gratings have been machined onto a metallic substrate using 5 axis diamond machines. Another technique involving argon ion etching of a freeform flexible

Further author information: (Send correspondence to cyril.bourgenot@durham.ac.uk)

Sol-Gel replicated surface has also been described in Ref.¹⁵ Finally, future space instruments incorporating freeform gratings are currently being studied for LUVOIR¹⁶ or CHIMA.¹⁷

This paper discusses the opportunities offered by this new type of dispersive elements to be used in a compact multi-channel hyperspectral imager and the progress made at Durham University in the production of these surfaces. The section 2 discusses the advantages and limitations of metallic diamond machined freeform gratings using commercial machines to rule the grating's lines. The section 3 describes the design concept of an EO instrument and the opportunities offered by freeform gratings. Section 4 describes the prototype design while section 5 compares the suitability of Nickel phosphorus (NiP) and RSA 6061 as a material substrate to achieve the lowest roughness and the sharpest groove profile.

2. ADVANTAGES AND LIMITATION OF SINGLE POINT DIAMOND MACHINED GRATINGS

Durham University is equipped with two Moore Nanotech Freeform Generator 5 axis diamond machines. At least 4 axis are needed for the machining of freeform gratings: 3 linear axes (X, Y and Z) to follow the shape of the freeform substrate, and an additional angular axis (B) to enable the rotation of the diamond tool and to produce a constant blaze angle on a curved surface. This technology offers several advantages over competing technologies:

- Single or multiblaze structures can be machined to optimize the efficiency at respectively one or multiple wavelengths. Therefore, multiblaze maximizes the diffraction efficiency over a larger spectral range. 5 axes diamond machines can also be used to produce variable spaced grooves to take into account and compensate the projection effect of the grating's lines on a curved surface.
- There is practically no limitations in the shape of the substrate which can be achieved by standard CNC machining or 3D printing capability. Metallic substrates can be easily light weighted, fitted with tapped holes and/or positioning pins directly into the component. In addition, the parts can be machined in their vertical operational positions.
- Cryogenic applications require resistant and thermally stable substrates. With the emergence of new alloys such as Nickel's coefficient of thermal expansion (CTE) matched aluminum alloy (RSA 443 from RSP technology), fine microstructure aluminum RSA 6061, or RSA 905, different parts of a spectrograph can be made in the same material with no or minimal bi-material effect.
- It is possible to machine steep and large sag surfaces.
- Finally, the programming and machine setup are relatively straightforward, making this technology cost effective.

Although there are obvious benefits in the production of diamond ruled freeform gratings with commercial machines, there are also 2 main limitations:

- Tool wear: As the same tip of the diamond tool is used to scribe all the gratings' lines, tool wear can affect the homogeneity of the groove profile and subsequently the efficiency. This effect is increased on large surfaces or with a higher groove frequency.
- Thermal effect: Thermal variations occurring during machining, induce a variation of surface form and ultimately a distortion of the wavefront. This effect is also increased for long cutting time.

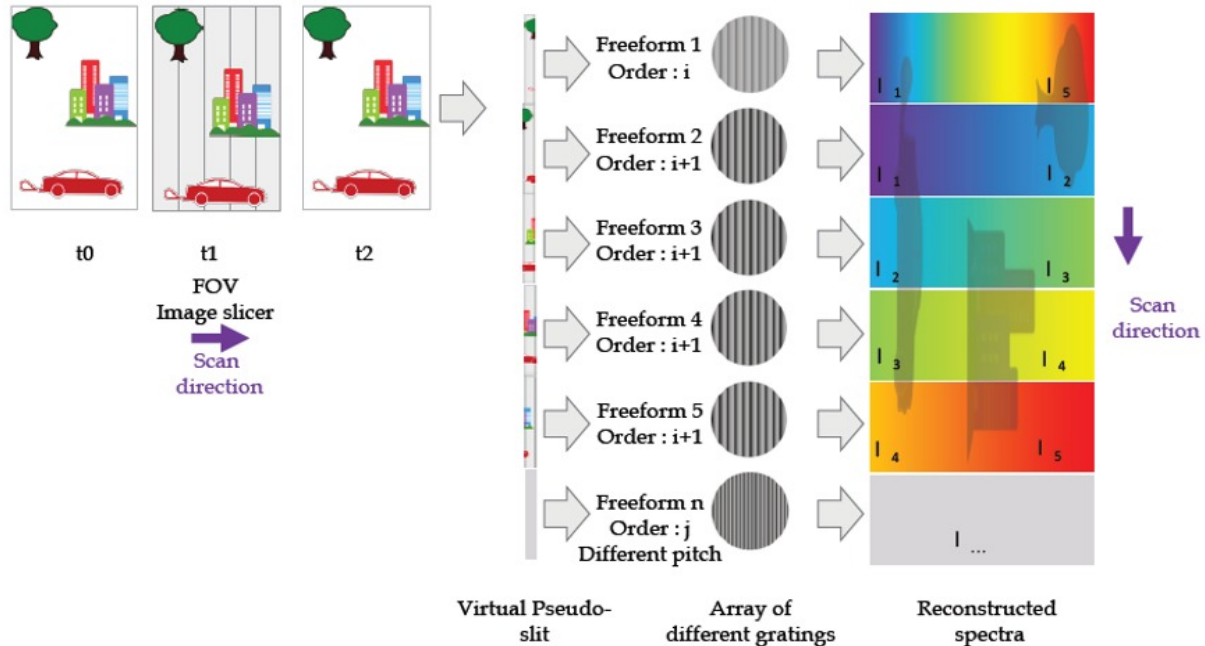


Figure 1: Concept of an ultra-compact multi-channel imaging spectrograph using a slicer mirror and an array of freeform gratings. The light from the scene is collected through a telescope and an image is formed on an image slicer. Each slice maps the same area on the ground sequentially and relays the light onto a specific grating for a tailored spectral analysis.

3. COMPACT MULTICHANNEL HYPERSPPECTRAL IMAGER

Integral Field Spectrograph (IFS) based on image slicers have the benefit of offering an extra dimension in the build-up of hyperspectral imaging data compared to traditional pushbroom slit spectrometers.¹⁸ This extra dimension, which in essence is substantiated by the number of image slices N , can be used to increase the sensitivity of the instrument or to increase the number of simultaneous wavelength channels.¹⁹ A concept of an image slicer based IFS is presented in this paper utilizing blazed metallic freeform gratings as the dispersive element as shown on Figure 1. This design will suit remote sensing missions, which require a number of spatial or spectral bands, whilst simultaneously offering compactness, high spatial/spectral resolution and modularity. The airborne platform's motion induces a pushbroom scan of the scene which is then reimaged onto the slicer mirror. Each slice sequentially redirects the light from the same portion of the scene onto a specific freeform grating, which acts as a disperser and a re-imager onto the sensor. The gratings' arrangement into a compactly packed array is optimized to reformat the image slicer into a virtual pseudo slit. Each grating is optimized to probe a specific spectral domain, at a defined spectral resolution, while the spatial resolution remains the same for all gratings.

Commercial hyperspectral systems usually have a broad wavelength bandwidth²⁰ to widen the range of application and this broad spectral window is not always fully used, potentially leading to extra weight and data processing. Hyperspectral data collected over a large number of narrow bands in continuous spectral coverage are voluminous and complex, posing great challenges in data handling and analysis.²¹ This design will allow data collection exclusively on selected spectral bands, enabling a more efficient data reduction.

4. FREEFORM GRATING PROTOTYPE DESIGN

A spectrograph prototype composed of a single freeform grating was designed and machined. The system specifications are given in Table 1, and were inspired from previous experience on¹³. The main optical element is a freeform surface which is an off axis, tilted ellipse, working at magnification 1:1. The clear aperture is

$\Phi 45\text{mm}$, and the grating has a line density of 100 lines/mm. The grating is optimized to work at diffraction order 1, and over the visible wavelength range so to make it compatible with existing metrology instrument at Durham University working in the visible. In the diffraction limited regime, the theoretical spectral resolution is consequently 4500.

Table 1: prototype optical specification

slicer dimension (FOV)	4mm x 0.1mm
Diameter	45mm
Magnification	1.0
F number	F/6.6
Grating definition	100 lines / mm
Wavelength range	400nm 700nm
Radius of curvature	300mm
Off axis angle	1.2°

The layout is given on Figure 2(a). The beam path is folded to separate the input beam from the spectrally dispersed output. The prototype is optimized to be used with a 10 microns core optical fiber as the object. The fiber can also be replaced by a slit or slice whose axis is aligned along the normal to the plane of the drawing. Figure 2(b) shows what would be the Modulation Transfer Function (MTF) for a spherical grating. The Point Spread Function (PSF), mostly affected by astigmatism because of the off-axis beam, is also displayed. Figure 2(c) shows the near diffraction limited performances offered, this time, by a freeform surface (tilted ellipse section). There is a 6- fold gain in the spectral resolution.

5. ROUGHNESS MEASUREMENT CHOICE OF BEST MATERIAL

Four freeform gratings have been machined at Durham University's Precision Optics Laboratory, according to the specifications presented in Table 1. Further to these specifications, the gratings also have the following individual characteristics:

- Grating 1 was machined in Aluminum RSA 6061 with a constant line frequency optimized for a maximum efficiency at 588nm (blaze angle 1.68°).
- Grating 2 was machined in Aluminum RSA 443 and plated with NiP, with a constant line frequency optimized for wavelength 588nm.

Grating 1 and 2 were compared in terms of groove profile quality and roughness, and the best material was selected for gratings 3&4. NiP was identified as the substrate offering the best roughness and profile quality. The comparison between RSA 6061 and NiP is discussed in the following.

- Grating 3, in RSA 443+NiP substrate, was machined with a dual blazed structure, optimized for wavelengths 470nm (blaze angle 1.3°) and 1047nm (blaze angle 3°).
- Grating 4, in RSA 443+NiP substrate, was machined with a variable period, optimized for a maximum efficiency at 588nm. The variation between the period at the center and edge of the grating aperture was about 20 nanometers.

The 4 gratings are shown in Figure 3. The roughness and the quality of the groove profile have been measured and compared on gratings 1 & 2. 300 grooves were measured on each gratings, using a Zygo Newview Whitelight interferometer equipped with a x10 objective (internal magnification x1.3). The best fit fourth order polynomial was removed from the data and the RMS roughness was measured on the processed data. The histogram is

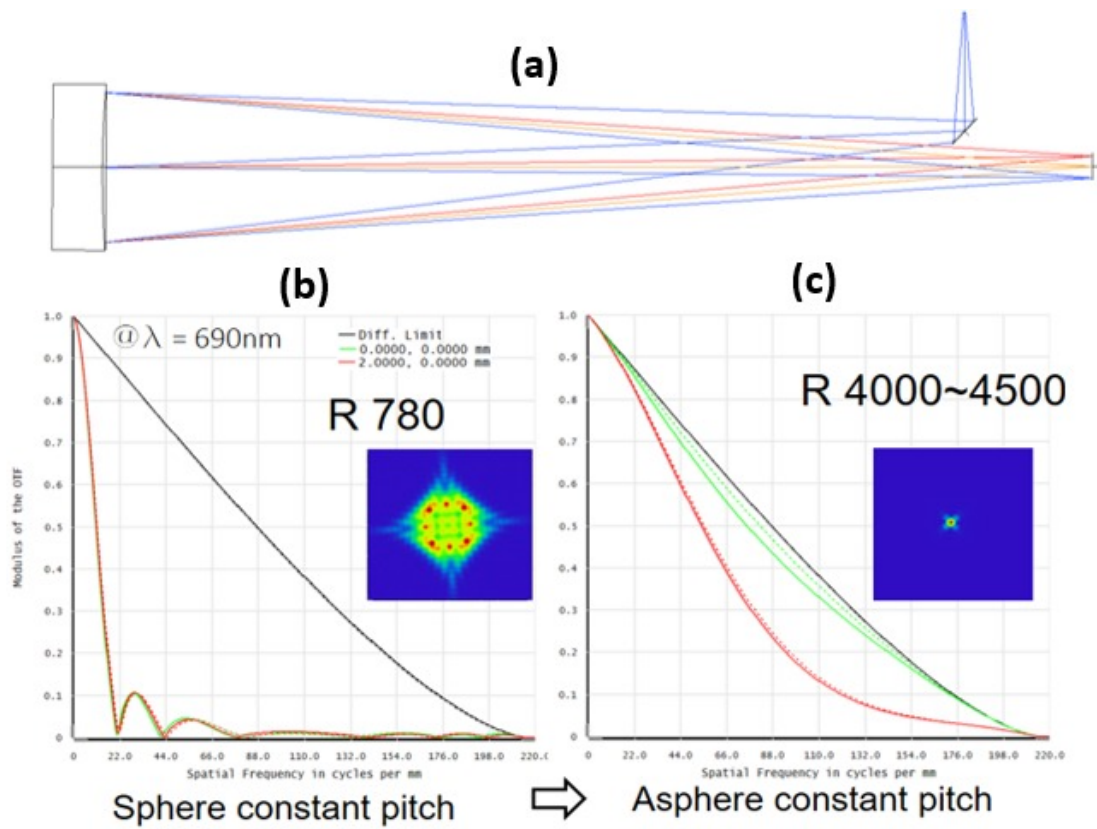


Figure 2: Concept of an ultra-compact multi-channel imaging spectrograph using a slicer mirror and an array of freeform gratings. The light from the scene is collected through a telescope and an image is formed on an image slicer. Each slice maps the same area on the ground sequentially and relays the light onto a specific grating for a tailored spectral analysis.



Figure 3: 4 freeform diffraction gratings machined according to the specification in Table 1.

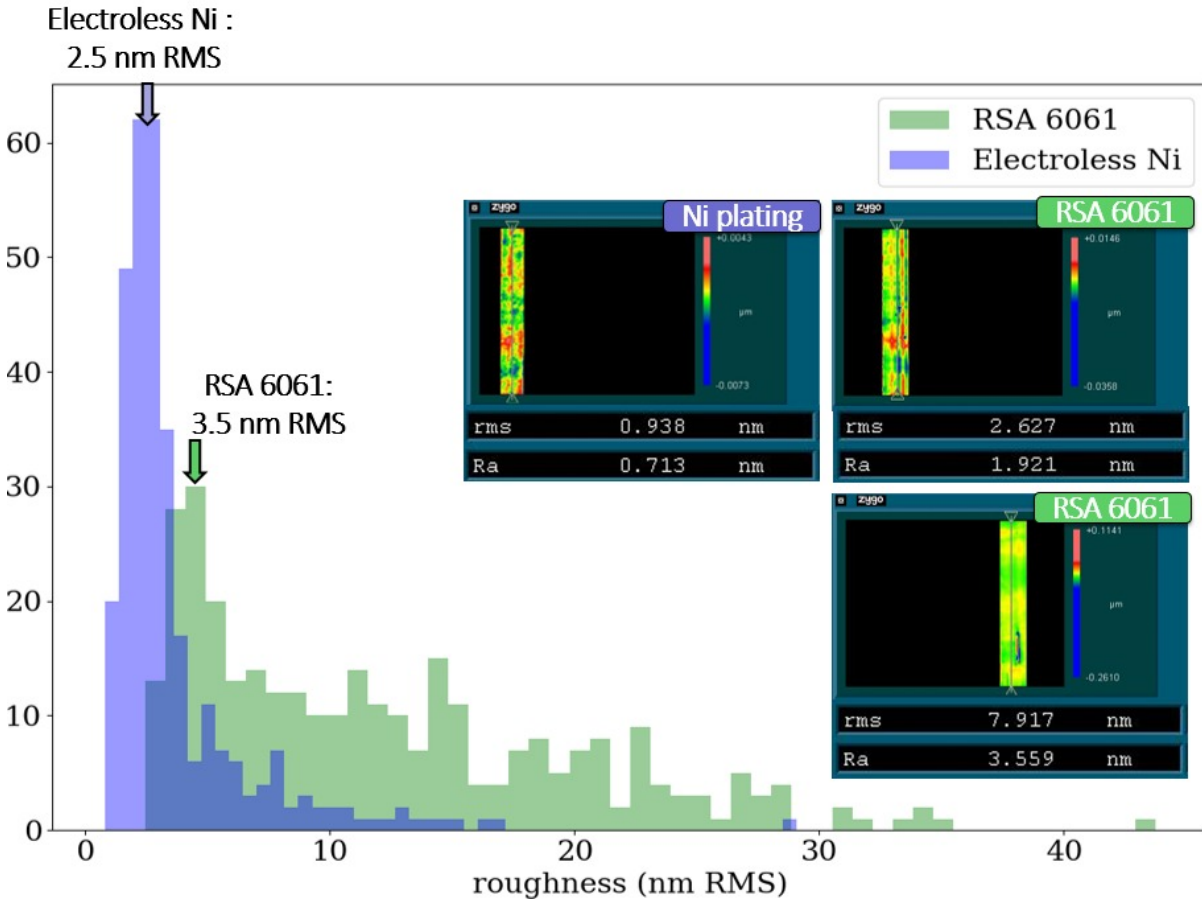


Figure 4: Histograms showing the RMS roughness measured on ruled gratings with substrate in NiP (purple), and RSA 6061 (green). Images of typical surface textures are given for NiP and RSA 6061 (top). The bottom image shows a distinctive line on the surface, which strongly affects the roughness on RSA 6061. Similar issues are not observed on NiP, which has a more homogeneous composition.

shown in Figure 4. NiP is the material offering the lowest roughness RMS with a histogram peaking at 2.5nm RMS while RSA 6061 is at 3.5nm RMS. One noticeable feature is the spread of the RSA 6061 histogram, which reveals that there is a larger variability between grooves for this material. The reason for this roughness heterogeneity between each facet is explained by the fact that some of the harder elements in the aluminum alloy, are occasionally dragged along the line, significantly affecting the roughness. The typical groove profiles measured on both NiP and RSA 6061 are shown on Figure 5. The profile machined on NiP is sharper. It was found that the profile was mainly limited by the tool local waviness and shape (less than 8nm PV). RSA 6061, on the other hand, presents a raised section at the edge of the groove. RSA 6061 is a much softer material than nickel, and as the tool scribes the grating's line, it locally distorts the narrowest and more fragile section of the groove. This issue will likely affect the efficiency of the grating.

6. CONCLUSION

This paper presents the ongoing machining tests at Durham University to produce freeform gratings using commercial 5 axis diamond machines. A new concept of multichannel hyperspectral imager, for pushbroom scanning platforms, based on an array of freeform gratings has been described. This type of design, inspired by image slicer based integral field spectroscopy, will offer multiband capability on a compact and modular system. The paper has compared the performance of 2 materials, NiP and bare aluminium RSA6061 in terms of

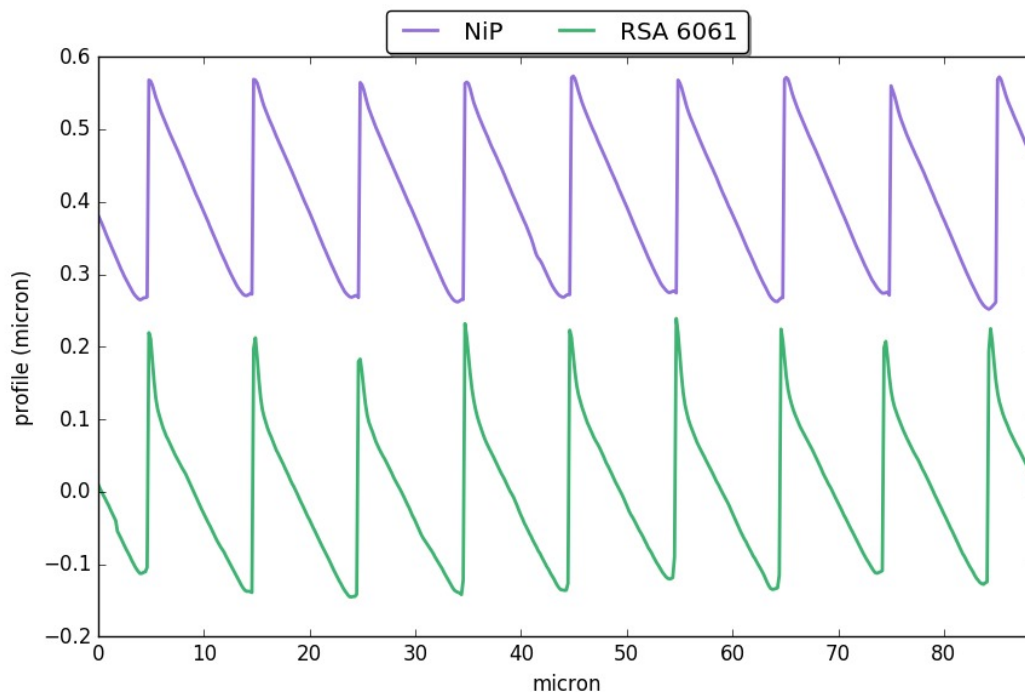


Figure 5: Typical groove profile for NiP material (purple) and Aluminum RSA 6061 (green). The best profile quality is obtained on NiP. RSA 6061 exhibits some distortion at the edge of the groove.

roughness and the shape of its groove. NiP offers an average roughness of 2.5nm RMS per facet, and a sharper profile with no obvious irregularities other than the one created by the local tool waviness.

Acknowledgements

We acknowledge receipt of support from the Centre of Earth Observation Instrumentation (CEOI) 10th Open Call (Pathfinder).

REFERENCES

1. R. Tamai, M. Cirusuolo, B. Koehler, and M. Tuti, "The E-ELT program status,"
2. L. Simard, B. Ellerbroek, R. Bhatia, M. Radovan, and E. Chisholm, "Thirty Meter Telescope science instruments: a status report," **9908**, p. 99081V, 2016.
3. P. J. McCarthy, J. Fanson, R. Bernstein, D. Ashby, B. Bigelow, N. Boyadjian, A. Bouchez, E. Chauvin, E. Donoso, J. Filgueira, R. Goodrich, F. Groark, G. Jacoby, and E. Pearce, "Overview and status of the Giant Magellan Telescope Project," **9906**, p. 990612, 2016.
4. N. Thatte, M. Tecza, F. Clarke, R. L. Davies, A. Remillieux, R. Bacon, D. Lunney, S. Arribas, E. Mediavilla, F. Gago, N. Bezawada, P. Ferruit, A. Fragoso, D. Freeman, J. Fuentes, T. Fusco, A. Gallie, A. Garcia, T. Goodsall, F. Gracia, A. Jarno, J. Kosmalski, J. Lynn, S. McLay, D. Montgomery, A. Pecental, H. Schnetler, H. Smith, D. Sosa, G. Battaglia, N. Bowles, L. Colina, E. Emsellem, A. Garcia-Perez, S. Gladysz, I. Hook, P. Irwin, M. Jarvis, R. Kennicutt, A. Levan, A. Longmore, J. Magorrian, M. McCaughrean, L. Origlia, R. Rebolo, D. Rigopoulou, S. Ryan, M. Swinbank, N. Tanvir, E. Tolstoy, and A. Verma Aprajita, "HARMONI: a single-field wide-band integral-field spectrograph for the European ELT," *Proc. SPIE* **7735**(July), p. 12, 2010.

5. P. J. McGregor, G. J. Bloxham, R. Boz, J. Davies, M. Doolan, M. Ellis, J. Hart, D. J. Jones, L. Luvaul, J. Neilsen, S. Parcell, R. Sharp, D. Stevanovic, and P. J. Young, "GMT Integral-Field Spectrograph (GMTIFS) conceptual design," (March), 2012.
6. D. L. DePoy, R. Allen, R. Barkhouser, E. Boster, D. Carona, A. Harding, R. Hammond, J. L. Marshall, J. Orndorff, C. Papovich, K. Prochaska, T. Prochaska, J. P. Rheault, S. Smee, S. Sheckman, and S. Villanueva, "GMACS: a wide field, multi-object, moderate-resolution, optical spectrograph for the Giant Magellan Telescope," *Proc. SPIE 8446, Ground-based and Airborne Instrumentation for Astronomy IV* **8446**(March), p. 84461N, 2012.
7. B. R. Brandl, R. Lenzen, E. Pantin, A. Glasse, J. Blommaert, L. Venema, F. Molster, R. Siebenmorgen, H. Boehnhardt, E. van Dishoeck, P. van der Werf, T. Henning, W. Brandner, P.-O. Lagage, T. J. T. Moore, M. Baes, C. Waelkens, C. Wright, H. U. Käufl, S. Kendrew, R. Stuik, and L. Jolissaint, "METIS: the Mid-infrared E-ELT Imager and Spectrograph," **14**(20), p. 70141N, 2008.
8. S. Lee, I.-S. Yuk, H. Lee, W. Wang, C. Park, K.-J. Park, M.-Y. Chun, S. Pak, J. Strubhar, C. Deen, M. Gully-Santiago, J. Rand, H. Seo, J. Kwon, H. Oh, S. Barnes, J. Lacy, J. Goertz, W.-K. Park, T.-S. Pyo, and D. T. Jaffe, "GMTNIRS (Giant Magellan Telescope near-infrared spectrograph): design concept," *Astronomy* **7735**, pp. 77352K–77352K–9, 2010.
9. J. E. Larkin, A. M. Moore, E. J. Barton, B. Bauman, K. Bui, J. Canfield, D. Crampton, A. Delacroix, M. Fletcher, D. Hale, D. Loop, C. Niehaus, A. C. Phillips, V. Reshetov, L. Simard, R. Smith, R. Suzuki, T. Usuda, and S. A. Wright, "The infrared imaging spectrograph (IRIS) for TMT: instrument overview," *Ground-based and Airborne Instrumentation for Astronomy III. Edited by McLean* **7735**, pp. 773529–773529–13, 2010.
10. A. Szentgyorgyi, J. Bean, B. Bigelow, A. Bouchez, M.-y. Chun, J. D. Crane, H. Epps, I. Evans, J. Evans, A. Frebel, G. Furesz, A. Glenday, D. Guzman, T. Hare, B.-h. Jang, J.-g. Jang, U. Jeong, A. Jordan, K.-m. Kim, J. Kim, C.-h. Li, M. Lopez-morales, K. Mc, B. Mcleod, M. Mueller, J. Nah, T. Norton, H. Oh, J. Sok, M. Ordway, B.-g. Park, C. Park, S.-j. Park, and S. E. Ave, "A Preliminary Design for the GMT-Consortium Large Earth Finder," *Society of Photo-Optical Instrumentation Engineers (SPIE) Conference Series* , pp. 1–16, 2014.
11. B. Barbuy, V. Bawden Macanhan, P. Bristow, B. Castilho, H. Dekker, B. Delabre, M. Diaz, C. Gneiding, F. Kerber, H. Kuntschner, G. La Mura, W. Maciel, J. Meléndez, L. Pasquini, C. B. Pereira, P. Petitjean, R. Reiss, C. Siqueira-Mello, R. Smiljanic, and J. Vernet, "CUBES: cassegrain U-band Brazil-ESO spectrograph," *Astrophysics and Space Science* **354**(1), pp. 191–204, 2014.
12. K. P. Thompson and J. P. Rolland, "Freeform Optical Surfaces: A Revolution in Imaging Optical Design," *Optics and Photonics News* **23**(6), p. 30, 2012.
13. C. Bourgenot, D. J. Robertson, D. Stelter, and S. Eikenberry, "Towards freeform curved blazed gratings using diamond machining," **9912**, p. 99123M, 2016.
14. R. Steiner, A. Pesch, L. H. Erdmann, M. Burkhardt, A. Gatto, R. Wipf, T. Diehl, H. J. P. Vink, B. van den Bosch, B. Sabushimike, G. Horugavye, P. Piron, V. Moreau, S. Habraken, B. Pptrp, V. Moreau, C. D. Clercq, A. Z. Marchi, J.-f. J.-f. Jamoye, S. Habraken, L. Maresi, V. Moreau, B. Delaure, C. Coolen, L. De Vos, D. Lee, J. Barlow, A. Vick, P. Hastings, D. Atkinson, M. Black, S. Wilson, P. I. Palmer, C. Islands, R. Navarro, L. Venema, I. Introduction, HYSPIRI, B. Guldinann, A. Deep, R. Vink, J. Ge, D. Q. Ren, J. I. Lunine, R. H. Brown, R. V. Yelle, L. A. Soderblom, R. Doe, S. Watchorn, J. Noto, R. Kerr, K. V. Dyk, K. Leveque, C. Sioris, M. Cutter, S. M. Sweeting, L. E. Comstock, R. L. Wiggins, C. D. Clercq, V. Moreau, J.-f. J.-f. Jamoye, A. Zuccaro, L. S. Park, C. Ardennais, B. Angleur, R. Casini, P. G. Nelson, C. Bourgenot, D. J. Robertson, D. Stelter, S. Eikenberry, R. K. Bean, and J. D. Pierce, "ELOIS : an innovative spectrometer design using a free-form grating," *Presentation* **31**(4), pp. 2179–2184, 2015.
15. F. Zamkotsian, P. Spano, P. Lanzoni, H. Ramarijaona, M. Moschetti, M. Riva, W. Bon, L. Nicastro, E. Molinari, R. Cosentino, A. Ghedina, M. Gonzalez, P. Di Marcantonio, I. Coretti, R. Cirami, F. Zerbi, and L. Valenziano, "BATMAN: a DMD-based multi-object spectrograph on Galileo telescope," **914713**(July 2014), p. 914713, 2014.
16. E. Muslimov, M. Ferrari, E. Hugot, J.-c. Bouret, C. Neiner, S. Lombardo, G. Lemaitre, R. Grange, E. Muslimov, M. Ferrari, E. Hugot, J.-c. Bouret, C. Neiner, E. R. Muslimov, M. Ferrari, E. Hugot, J.-c. Bouret, and C. Neiner, "Spectrographs with holographic gratings on freeform surfaces : design approach and application

for the LUVOIR mission To cite this version : HAL Id : hal-01796075 Spectrographs with holographic gratings on freeform surfaces : design approach and applicati,” 2018.

17. V. Moreau and A. Z. Marchi, “FreeForm Gratings for Imaging Spectrometers Turn-key Telescopes,” 2017.
18. R. Content, S. Blake, C. Dunlop, D. Nandi, R. Sharples, G. Talbot, T. Shanks, D. Donoghue, N. Galiatsatos, and P. Luke, “New Microslice Technology for Hyperspectral Imaging,” *Remote Sensing* **5**(3), pp. 1204–1219, 2013.
19. D. Lee, J. Barlow, A. Vick, P. Hastings, D. Atkinson, M. Black, S. Wilson, and P. I. Palmer, “PERSIST: prototype Earth observing system using image slicer mirrors,” in *Proc. SPIE 8533, Sensors, Systems, and Next-Generation Satellites XVI*, ; doi:10.1117/12.973752., R. Meynart, S. P. Neeck, and H. Shimoda, eds., p. 85330T, nov 2012.
20. T. Adão, J. Hruška, L. Pádua, J. Bessa, E. Peres, R. Morais, and J. J. Sousa, “Hyperspectral imaging: A review on UAV-based sensors, data processing and applications for agriculture and forestry,” *Remote Sensing* **9**(11), pp. 1–31, 2017.
21. R. N. Sahoo, S. S. Ray, and K. R. Manjunath, “Hyperspectral remote sensing of agriculture,” *Current Science* **108**(5), pp. 848–859, 2015.